Calculation of Lightning and Switching Overvoltages Transferred through Power Transformer

Bruno Jurišić, Tomislav Župan, Mario Jurić, Božidar Filipović-Grčić, Katarina Musulin

Abstract — **During their lifespan all primary HV equipment installed in the power system is subjected to transients. Therefore, it is necessary to adequately dimension and protect the equipment. However, in the networks with high share of renewables, power electronics, cables or near gas insulated substation (GIS), the failure can occur even though good practices of insulation coordination are fulfilled.**

In this paper, a high-frequency power transformer model is presented. Such model is based on measurements of admittance matrix and is adequate for simulation of fast front transients in EMTP like software. Additionally, simulations of transferred lightning and switching overvoltages are given for the observed power transformer unit.

Keywords — **fast front transients, power transformer, EMTP, measurement, admittance matrix**

I. Introduction

In everyday operation, power transformers are exposed to switching and lightning overvoltages. Overvoltages that are experienced by the transformer and other HV equipment inside substation can be estimated and calculated using advanced simulations in software tools for calculating transient phenomena, for example ElectroMagnetic Transients Program (EMTP) [1]. Such simulations imply the use of advanced high-frequency transformer models and frequency-dependent models of other HV equipment in the substation.

Advanced transformer models are necessary to simulate fast and very fast overvoltages in the power system [2], [3]. Due to the significant share of high frequencies in such overvoltages, resonant phenomena may occur within the windings of the power transformer, which can endanger its dielectric insultation. For this

reason, on-line monitoring systems for measurement of overvoltages can be installed and usually they are connected over measuring tap of transformer bushing [4], [5]. The electromagnetic behaviour of the transformer at its terminals is a function of these resonant phenomena. Consequently, traditional transformer models, made primarily for the nominal operating frequency (50 Hz or 60 Hz), are not accurate enough to simulate such transient phenomena [6].

According to CIGRE research [7], the majority of power transformer failures have an unknown cause. Therefore, it is necessary to pay particular attention when protecting such an object, because standard transformer tests do not cover all phenomena and conditions in which the transformer can be found in the network. Particularly noteworthy are resonant overvoltages, where transformer protection with surge arresters is not effective. Examples of faults, caused by the interaction of the transformer and electric power network, are given in the CIGRE brochure [8].

In this paper, a high-frequency power transformer model is presented. The second chapter describes a method for measuring the frequency-dependent admittance matrix of the transformer. The third chapter explains the transformer model developed in the software tool for the calculation of transient phenomena. Verification of the model using the measurement results in the time domain is described in the fourth chapter. Examples for the calculations of possible transient phenomena due to lightning strikes or switching operations are given for the considered power transformer in the fifth chapter. Conclusions are given in the chapter six.

II. Method for Measuring the Frequency-dependent Admittance Matrix of the Transformer by Measuring the Voltage Ratios

Below is a procedure for measuring the admittance matrix using the capabilities of the Vector Network Analyzer (VNA) device to measure the ratio of input and output voltage. Such a device corresponds to the Sweep Frequency Response Analysis (SFRA) device, which is a part of the standard measurement equipment in every high-voltage laboratory. This kind of measurement can also be carried out in the field, in the transformer substation.

The procedure for measuring the transformer admittance matrix with the VNA device is based on the following expressions [9] -[11]:

$$H_{voltage}(s) = \frac{V_{out}(s)}{V_{in}(s)} \qquad (1)$$

(Corresponding author: Bruno Jurišić)

Bruno Jurišić and Tomislav Župan are with the KONČAR - Electrical Engineering Institute Ltd., Zagreb, Croatia
(e-mail: bjurisic@koncar-institut.hr, tzupan@koncar-institut.hr)

Mario Jurić is with the Croatian Transmission System Operator Ltd., Zagreb, Croatia
(e-mail: mario.juric@hops.hr)

Božidar Filipović-Grčić is with the University of Zagreb Faculty of electrical engineering and computing, Zagreb, Croatia
(e-mail: bozidar.filipovic-grcic@fer.hr)

Katarina Musulin is with the Ravel Ltd., Zagreb, Croatia
(e-mail: katarina.musulin@ravel.hr)

$$\begin{pmatrix} I_1 \\ I_2 \\ \vdots \\ I_{N-1} \\ I_N \end{pmatrix} = \begin{pmatrix} Y_{11} & \cdots & Y_{1N} \\ \vdots & \ddots & \vdots \\ Y_{N1} & \cdots & Y_{NN} \end{pmatrix} \cdot \begin{pmatrix} V_1 \\ V_2 \\ \vdots \\ V_{N-1} \\ V_N \end{pmatrix}, \qquad (2)$$

,

where:

H_{voltage} is ratio of measured input voltage V_{in} and output voltage V_{out}.

The circuit for measuring the admittance matrix differs for diagonal and off-diagonal coefficients of the matrix. Two measurement circuits are shown in the figures below considering a 300 MVA YNa0d5 autotransformer as a test object, which has 10 or 11 terminals, depending on whether the tertiary winding is short- or open-circuited.
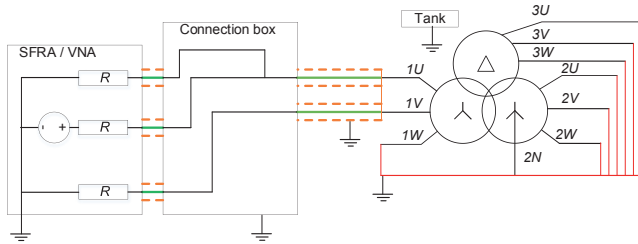

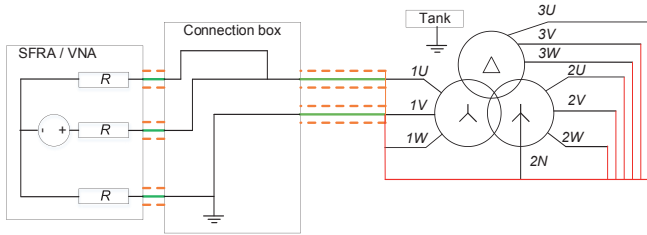Fig. 1: Circuit for measuring off-diagonal coefficients of the admittance matrix.

Fig. 2: Circuit for measuring diagonal coefficients of the admittance matrix.

Figures 1 and 2 show the equivalent scheme of the measuring equipment, which consists of three terminals: source, reference terminal and response measurement terminal. Each of the terminals is terminated with an impedance of 50 Ω, so that there are no reflections between the connected measuring cables (coaxial cable with a characteristic impedance of 50 Ω) and measuring device. The measuring device is set to measure the voltage ratio between the response measuring terminal and the reference terminal.

In all measurements it is necessary to maintain the grounding of the transformer tank.

Since the measurements are made in a high-voltage laboratory, the connection box is used only for grounding the coaxial cable shield. In the field, the connection box is used for easier handling and reconnection during measurement. Due to the limited possibilities and the unavailability of the bushing top, such a box drastically reduces the duration of the measurement. Such a box is not required for measurements in the laboratory, which reduces the number of cables used and thus increases the accuracy of the measurement.

In the figures above, the coaxial cables are marked in green while their electromagnetic shields are marked in orange. Copper strips used for the connection to the transformer cover are shown in

red. The connection between the measuring device and the connection box is made using short coaxial cables, while the connection between the connection box and the top of the transformer bushing is made using 18 meter long coaxial cables, which are part of the standard SFRA equipment.

Figure 1 shows the measurement of the admittance matrix element Y_{12} (between the terminals 1U-1V). All transformer terminals not involved in the measurement are short-circuited and grounded. In this way, from the expression for the admittance matrix (2) the following expression is obtained:

$$(3)$$
$$Y_{ij}(s) = -\frac{V_i(s)}{V_j(s)} \cdot \left(Y_{ii}(s) + \frac{1}{R} \right)$$

When measuring off-diagonal coefficients of the admittance matrix, all electromagnetic shields of the coaxial cables are short-circuited and grounded using wide copper strips at one end and a grounded aluminium connection box at the other end.

It is evident from expression (3) that each off-diagonal coefficient depends on the corresponding diagonal coefficient of the admittance matrix. In order to obtain admittance by measuring the voltage ratios, it is necessary to use the internal resistance of the response measurement terminal as a shunt resistor to measure the current. In this case, the diagonal coefficient of the admittance matrix can be calculated as:

$$Y_{ii}(s) = \frac{I_i(s)}{\left(V_{in}(s) - V_{out}(s) \right)} = \frac{V_{out}(s)}{R \cdot \left(V_i(s) - V_{out}(s) \right)} \qquad (4)$$

From figure 2 it can be seen that the measurement circuit is grounded before the measuring device so the current that closes through the transformer tank towards the measuring device contributes to the voltage drop on the internal resistance of the response measurement terminal. By doing this, all the sheaths of the coaxial cables must be short-circuited and left at the floating potential, so that the voltage drop across the internal resistance of the response measurement terminal is not equal to 0 V.

III. TRANSFORMER MODEL IN EMTP

The transformer model was created in the software for calculation of transients EMTP, using the semi definite programming (SDP) method for rational approximation, i.e. mathematical description of the model [12]. The frequency-dependent admittance matrix is described by rational functions with 60 poles. To exclude the noise from the measurements, an average filter (with a factor of 5) was used. Models have 10 terminals (1U, 1V, 1W, 2U, 2V, 2W, 2N, 3U, 3V, 3W). The results of the success of the mathematical model using rational functions are presented in the figures below. The deviation shown in the figures has been calculated as the amplitude difference between the measurement and the mathematical description of each coefficient.

The cumulative relative error of the mathematical description calculated using expression (5) is about 5%, which is consistent with the literature [12].

$$RMSRE = \sqrt{\frac{\sum_{i=1}^{N} \sum_{j=1}^{N} \sum_{k=1}^{N_k} \left(\left| \frac{Y_{ij}(f_k) - Y_{ij,fit}(f_k)}{Y_{ij}(f_k)} \right|^2 \right)}{N^2 * N_k}}, \qquad (5)$$

,

where:

N = number of transformer terminals,

f_k = frequency at which admittance matrix elements where measured,

N_k = number of frequency points,

Y_{ij} = measured transformer admittance matrix coefficient,

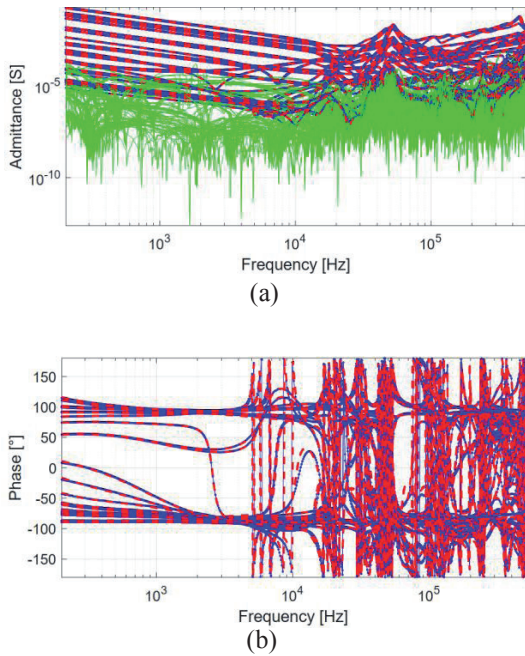$Y_{ij,fit}$ = mathematical description of transformer admittance matrix coefficient.

(a)

(b)

Fig. 3. Results of the rational approximation of the admittance matrix measured at nominal tap position (measured curves are marked in blue, the mathematical model in red, and the difference in green).
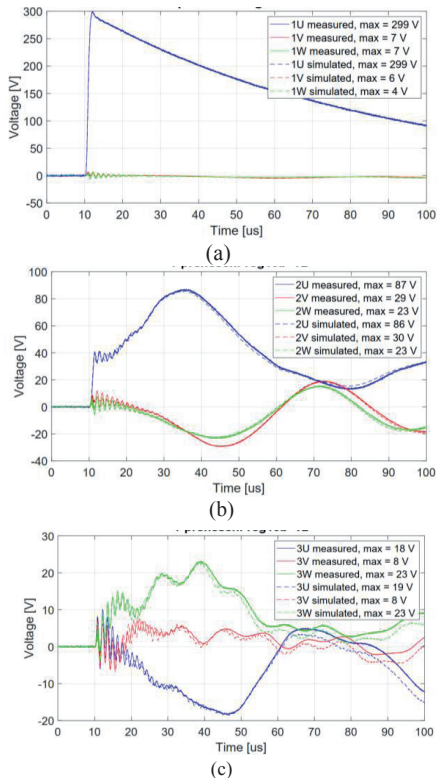
IV. VERIFICATION OF THE 300 MVA TRANSFORMER MODEL

This chapter presents a comparison of the results obtained by calculation of transients in the time domain and the results of the measured transferred overvoltages. The calculations are performed using EMTP, while the measurements are performed in the HV laboratory to minimize the influence of the environment and grounding as much as possible.

The measurements performed in this paper and are shown in the table 1. Standard (1.2/50 µs) lightning impulse (LI) is applied at terminal 1U in configuration 1, and at terminal 1V in configuration 2.

Transferred lightning overvoltage measurements are carried out for different combinations of R, L and C elements connected to the primary/secondary of the transformer, in order to verify the transformer models in the time domain and their behaviour when we consider a certain capacitance, inductance and resistance connected to the primary/secondary of the transformer, or when it is left open circuit (worst case for transferred overvoltages).

TABLE I.

MEASUREMENT CONFIGURATION FOR TRANSFERRED OVERVOLTAGES

Config-uration	1U	1V	1W	N	2U	2V	2W	3U	3V	3W
1	LI	R	R	grounded	iso-lated	iso-lated	iso-lated	iso-lated	iso-lated	iso-lated
2	R	LI	R	grounded	R	R	R	C	C	C

During the measurement, the voltages at all terminals of the transformer are observed. In table 1, R presents the characteristic impedance of the overhead transmission line (400 Ω), while C indicates the capacitance of the power cable (C ≈ 0.47 µF).

The figures below provide comparisons of the transformer model response and the measurement results.

The model was also verified at the nominal frequency of 50 Hz. The voltage waveforms as well as the voltage phasor display of the model are shown in the figure below.

(a)

(b)

(c)

Fig. 4. Measurement results of transmitted overvoltages for configuration 1, at nominal tap position
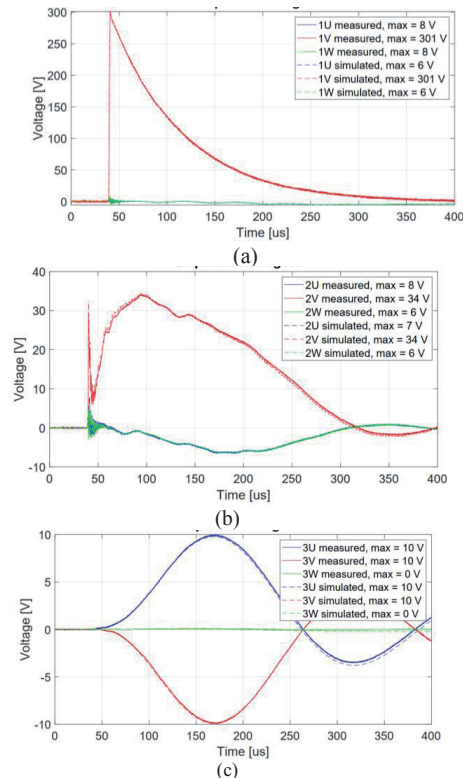

(a)

(b)

(c)

Fig. 5. Measurement results of transmitted overvoltages for configuration 2, nominal tap position
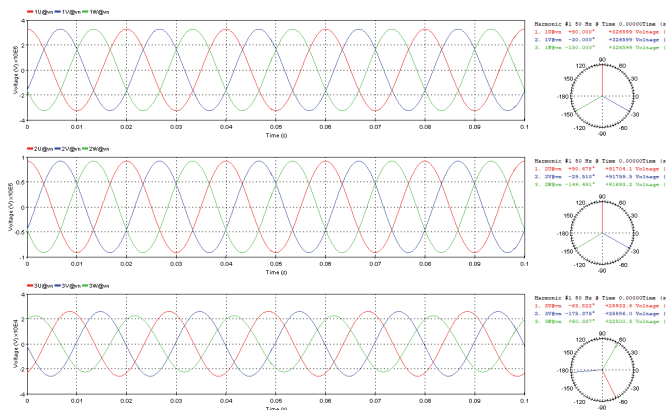
Fig. 6. Response model at 50 Hz, for nominal tap position

Values are additionally compared in table 2.

TABLE II.

COMPARISON OF NOMINAL AND CALCULATED VOLTAGES AT 50 HZ FOR NOMINAL TAP POSITION.

Winding	Phase	Nominal [kV]	Model [kV]	Rel. error [%]
Primary	a	220	220.0	-
	b	220	220.0	-
	c	220	220.0	-
Secondary	a	115	111.6	2.97
	b	115	111.6	2.96
	c	115	111.9	2.73
Tertiary	a	30	31.76	5.87
	b	30	31.70	5.68
	c	30	27.56	8.14

Increased relative error at tertiary side is caused by relatively low signal-to-noise ratio. Additionally, tertiary winding is delta connected and performing frequency response measurements is relatively demanding in the considered case. Even though the developed model is intended for high frequencies, relatively good results are also obtained for the operating frequency of 50 Hz.

V. SIMULATIONS OF TRANSFERRED LIGHTNING AND SWITCHING OVERVOLTAGES

Lightning overvoltages are calculated in the case of a lightning strike at 400 kV transmission line in the vicinity of an air-insulated substation where a 400/110/30 kV, 300 MVA, power transformer is installed. Detailed high-frequency models of transformer substation and connected transmission lines are developed in EMTP. Equivalent scheme of air-insulated substation considering reduced topology for calculations of transferred lightning overvoltages
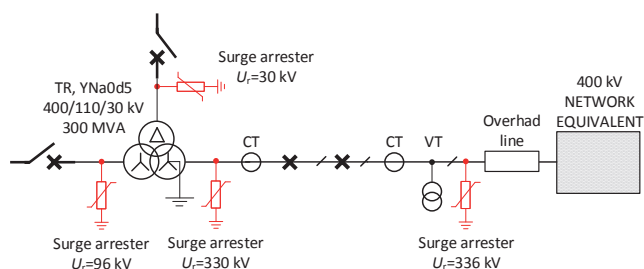
with indicated positions of surge arresters is shown in Fig. 7.

Fig. 7. Equivalent scheme of air-insulated substation considering reduced

topology for calculations of transferred lightning overvoltages with indicated positions of surge arresters.

Calculations are made with previously described high-frequency model of power transformer, which is created based on the frequency-dependent admittance matrix measurements. Transferred overvoltages are calculated at secondary and tertiary side of power transformer. An analysis of the effectiveness of the overvoltage protection is carried out and the resonant overvoltage phenomena are checked. Overvoltage calculation is based on the following conservative assumptions, according to which calculated values of lightning overvoltages should be higher than the ones that may occur in the reality:

- Substation operates with reduced topology – there are only one 400 kV transmission line bay and one transformer bay in operation. In this reduced topology, the overvoltage wave propagates directly towards the transformer, while in full topology it is distributed to the neighbouring 400 kV bays. Therefore, it is expected that with all the lines connected, the overvoltage amplitudes in the transformer bay will be lower.

- An extremely rare case of a 250 kA lightning strike at the second tower of the 400 kV transmission line from the entrance to the transformer substation is assumed, with tower grounding resistance of 10 Ω. In the second case, a direct 40 kA strike to the phase conductor is simulated. This "critical" current is obtained from electro-geometric model of the overhead line, and it represents the highest amplitude of the lighting strike that can hit the phase conductor directly. Lightning strikes with higher currents cannot directly hit the phase conductors due to the protection provided by the shield wires.

- At the moment of lightning strike, a state of increased operating voltage (420 kV) is assumed, which increases the probability of a backflashover occurrence.

- At the moment of lightning strike to 400 kV transmission line, 110 kV and 30 kV sides of power transformer are unloaded (open circuit breaker from 110 kV and 30 kV side). In this case, overvoltages that are transmitted to the secondary and tertiary transformer windings, and they are reflected on open contacts of circuit breaker. Reflected overvoltages travel back towards the transformer, so increased values of overvoltage can be expected in this case. The primary, secondary and tertiary sides of the transformer are protected by surge arresters (rated voltage of the surge arresters: U_r=330 kV, U_r=96 kV, U_r=38 kV).

A lightning strike causes a flashover in phase C, making it the phase in which the highest overvoltage is reached at the 400 kV transformer winding. Surge arresters in the 400 kV transformer bay limit the overvoltage to 836.6 kV. The calculated overvoltage waveforms are shown in figures 8-12. Figure 14 shows the measurement results of the magnitude and phase angle of admittance for 30 kV winding (phase B-C) as a function of frequency. The resonant frequencies of the 30 kV windings can be observed (approximately at the frequency of 52 kHz and 1,6 MHz) which differ from the dominant frequencies of the overvoltage oscillations (6.8 kHz), therefore it can be concluded that there is no risk of resonant overvoltages in 30 kV transformer windings (Fig. 13).
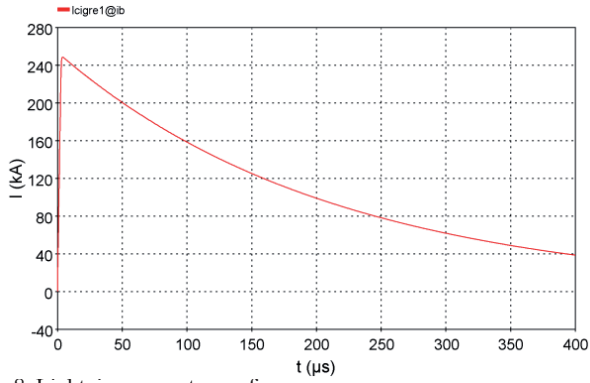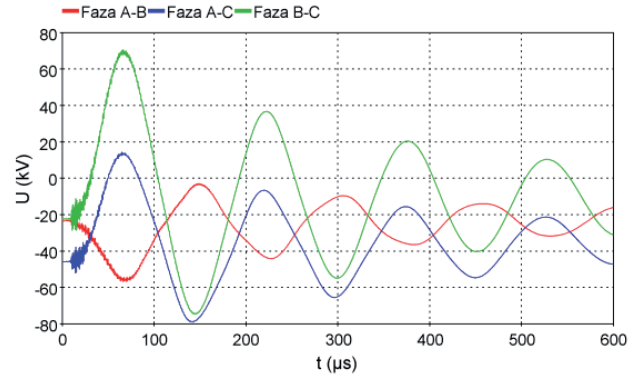
Fig. 8. Lightning current waveform.

Fig. 9. Flashover in phase C across the insulator string on tower struck by lightning.

Fig. 10. Overvoltages on the 400 kV side of the transformer (U_{max}=836.6 kV).
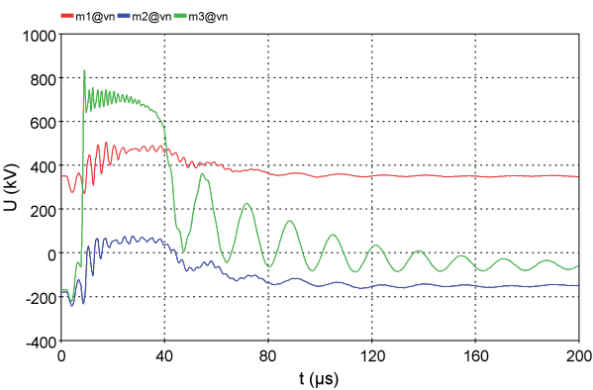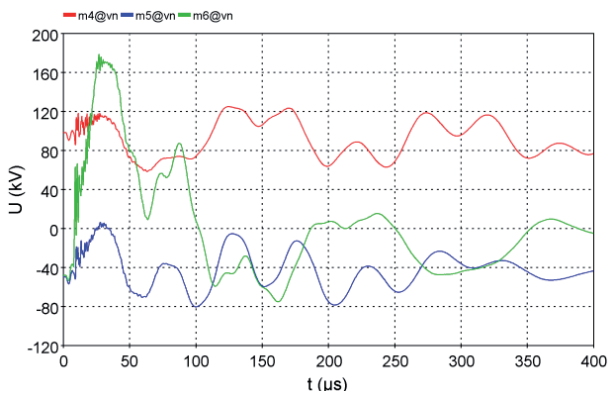

Fig. 11. Transferred overvoltages on the 110 kV side of transformer (U_{max}=178.7 kV).

Fig. 12. Transferred line overvoltages on 30 kV side of transformer (U_{max}=79.13 kV).

Fig. 13. Frequency spectrum of lightning overvoltage (phase B-C).

An overview of the calculation results is shown in the following table.

TABLE III.

OVERVIEW OF THE CALCULATION RESULTS OF LIGHTNING OVERVOLTAGES

	Lightning strike to the top of the tower	Lightning strike to the phase conductor
Lightning current amplitude	250 kA	40 kA
Overvoltages at the 400 kV side of the transformer	836.6 kV	838.2 kV
Transferred overvoltages on the 110 kV side of the transformer	178.7 kV	154.12 kV
Overvoltages on the open contact of the 110 kV circuit breaker 191.6 kV		196.9 kV
Transferred phase overvoltages on the 30 kV side of the transformer	48.17 kV	32.15 kV
Transferred line overvoltages on the 30 kV side of the transformer	79.13 kV	48.9 kV
Current through surge arresters in 400 kV overhead line bay	3.27 kA	13.8 kA
Surge arrester energy in 400 kV overhead line bay	18.62 kJ	9.15 kJ
Current through surge arresters in a 400 kV transformer bay	5. 05 kA	6.06 kA
Surge arrester energy in 400 kV transformer bay	69.9 kJ	6.6 kJ
Surge arrester energy in 110 kV transformer bay	96.5 J	0.87 kJ

Lightning overvoltage amplitudes for all elements of substation are within the permitted limits and they do not exceed the standard rated lightning impulse (1,2/50 µs) withstand voltages 1425 kV, 550 kV and 170 kV, which correspond to highest voltage for
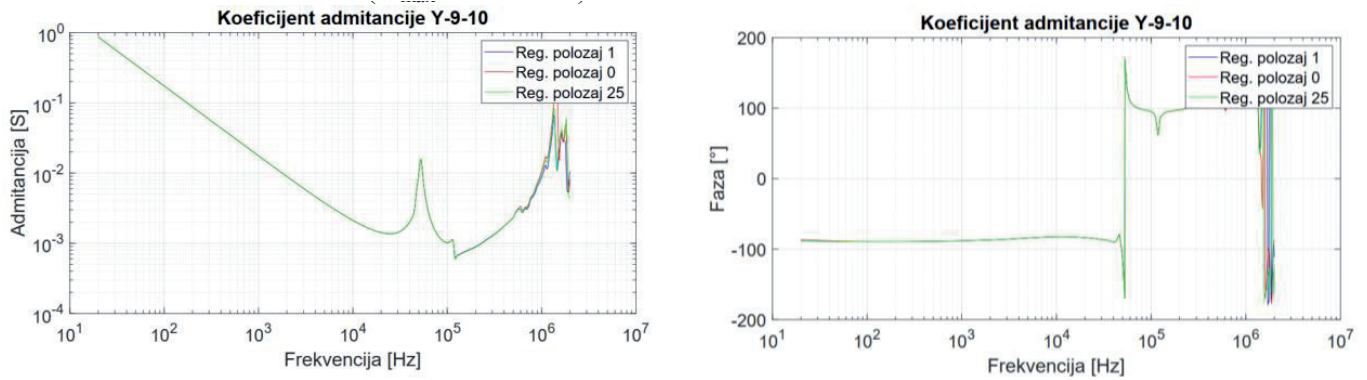
Fig. 14. Measurement results of a) amplitude and b) phase of the admittance of 30 kV winding (phase B-C).

equipment 400 kV 110 kV and 30 kV, respectively. Analysis of the frequency spectrum of the overvoltage and the frequency response of the transformer windings show that in the analysed cases there is no possibility of resonant overvoltages in the transformer winding. The energy stress of the surge arresters is within permitted limits. It is recommended to select the characteristics of the surge arresters in the line bay (U_r=336 kV) so that they correspond to the characteristics of the arresters in the transformer bay (U_r=330 kV). This would ensure better protection of equipment against overvoltages (mainly in the line bay) and the total energy stress would be distributed more evenly between surge arresters in the line bay and the transformer bay.

Transient phenomena during the switching of the vacuum circuit breakers in a 30 kV substation are analysed. Substation is connected on one side to a 400/110/30 kV power transformer via a 40 m long 30 kV cable and on the other side with a 200 m long 30 kV cable to a neighbouring 30 kV substation. In the neighbouring substation, there is a 30/0,4 kV distribution transformer with rated power of 1250 kVA. A detailed model of the 30 kV vacuum circuit breaker is developed in the EMTP for calculation of transient phenomena. Equivalent scheme of substation considering switching of vacuum circuit breaker in 30 kV network with indicated positions of surge arresters is shown in Fig. 15.
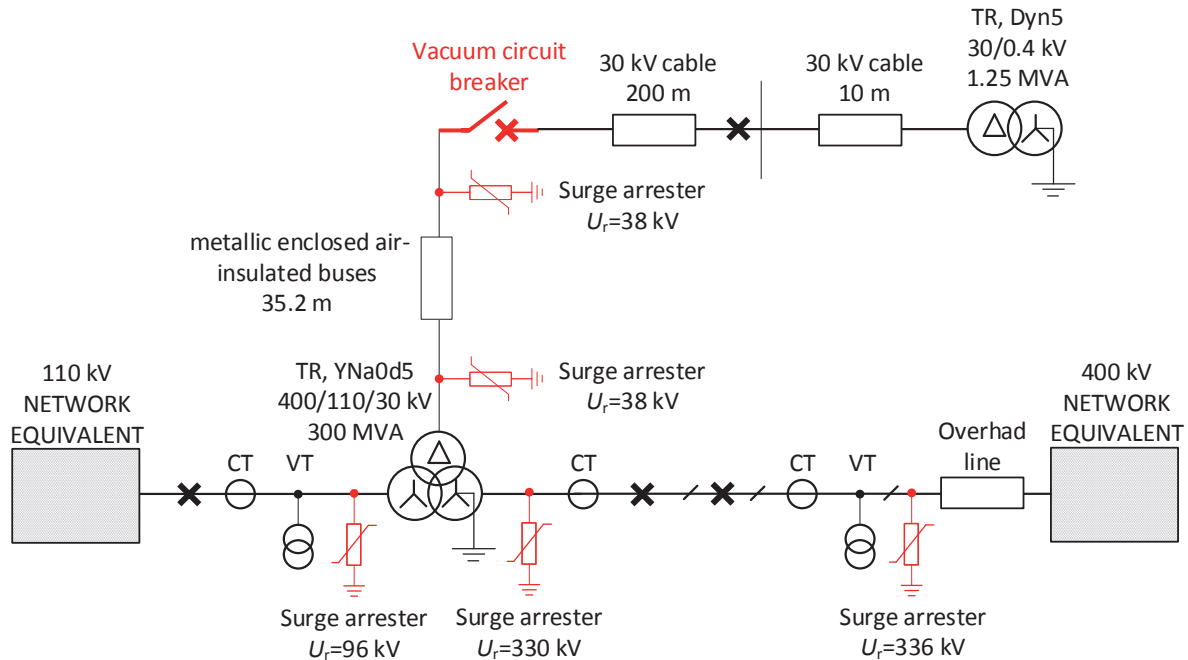

Fig. 15. Equivalent scheme of substation considering switching of vacuum circuit breaker in 30 kV network with indicated positions of surge arresters.

The model enables the simulation of restrikes that occur during the switching off a vacuum circuit breaker. Surge arresters (U_r=38 kV) are installed on the 30 kV side of the 400/110/30 kV power

transformer and at the entrance of the cable to the 30 kV substation, where vacuum circuit breakers and other equipment are located. Two cases are analysed:

- Case A): switching off 200 m long cable to the neighbouring 30 kV substation and an additional 10 m cable to 30/0,4 kV distribution transformer that is loaded with the nominal load.

- Case B): energization of the 200 m cable to the neighbouring 30 kV substation.

Figures 16-21 show the waveforms of the calculated overvoltages for case A. From the results it can be concluded that there is no risk of resonant overvoltages on the tertiary winding of the transformer due to the switching of vacuum circuit breaker.

TABLE IV.

OVERVIEW OF THE CALCULATION RESULTS − SWITCHING OFF THE VACUUM CIRCUIT BREAKER (CASE A)

Chopping current	Overvoltages at the end of a 200 m long 30 kV cable and at the distribution transformer	Transient recovery voltage on the vacuum circuit breaker	Frequency analysis of overvoltage on the transformer tertiary winding
15 A	U_{maxA}=77.85 kV U_{maxB}=50.64 kV U_{maxC}=88.75 kV	U_{maxA}=61.53 kV U_{maxB}=50.63 kV U_{maxC}=50.38 kV	HF spectrum of overvoltage: dominant frequency 566 kHz; LF overvoltage spectrum: dominant frequency 6.2 kHz

TABLE V.

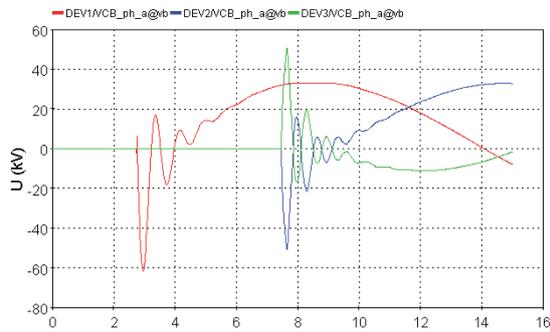OVERVIEW OF THE CALCULATION RESULTS − SWITCHING ON THE VACUUM CIRCUIT BREAKER (CASE B)

Inrush currents amplitudes	Switching overvoltages at the beginning and at the end of a 200 m long 30 kV cable	Frequency analysis of overvoltage on the transformer tertiary winding
I_{maxA}=581.4 A I_{maxB}=646.3 A I_{maxC}=582.9 A	Beginning: U_{maxA}=28.2 kV, U_{maxB}=28.7 kV, U_{maxC}=25.5 kV; End: U_{maxA}=46.8 kV, U_{maxB}=51.5 kV, U_{maxC}=46.3 kV	HF spectrum of overvoltage: dominant frequencies 784 kHz, 513 kHz and 1.145 MHz; LF overvoltage spectrum: dominant frequency 6 kHz

Fig. 16. Transient recovery voltage on the vacuum circuit breaker.
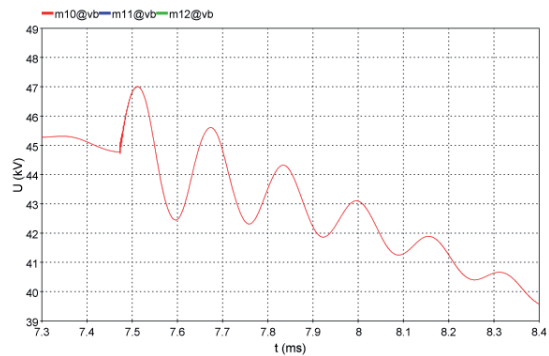

Fig. 17. Line voltages on the power transformer tertiary.

Fig. 18. Detail of overvoltage on the tertiary winding - dominant frequency after current breaking is approximately 6,2 kHz.

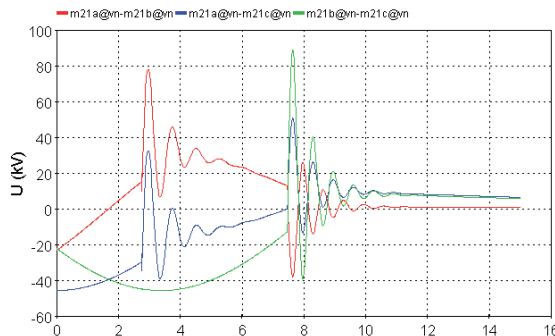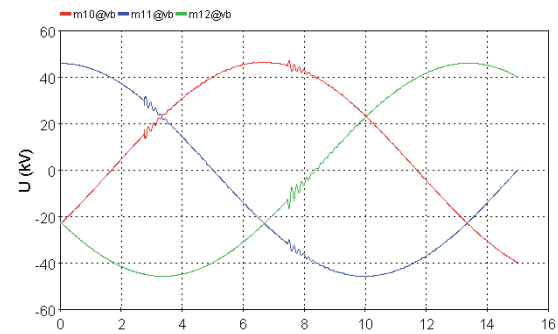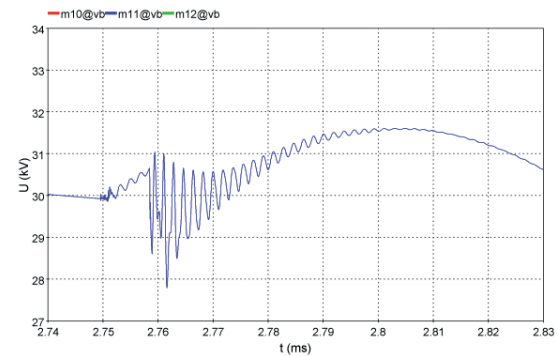Fig. 19. Detail of overvoltage on the tertiary winding - dominant frequency before current breaking during the transient recovery voltage is 566 kHz

Fig. 20. Line overvoltages on the HV side of the distribution transformer.
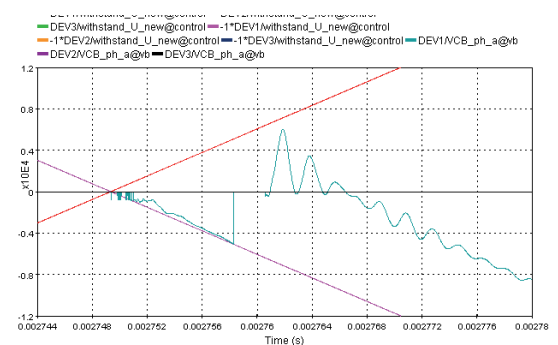

Fig. 21. Detailed view of the restrike on the circuit breaker terminals at the initial moment of the transient recovery voltage in phase A.

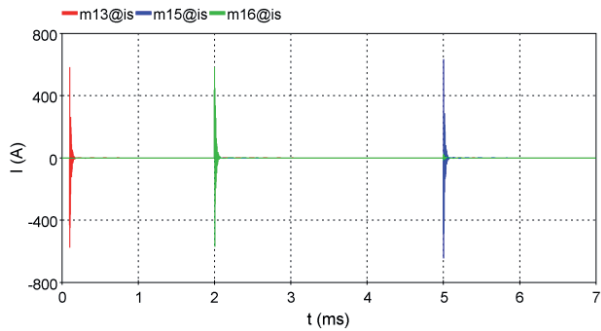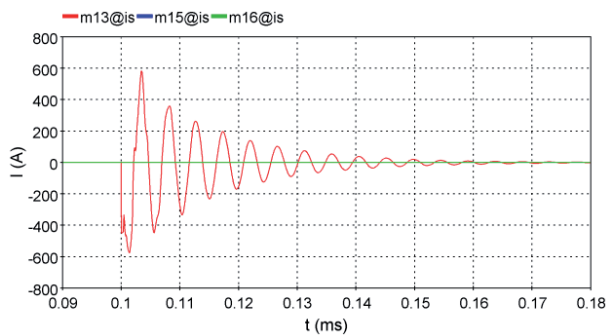Fig. 22. Inrush currents

Fig. 23. Switching overvoltages at the beginning and at the end of 30 kV cable

Fig. 24. Inrush current in phase A (instant of switching in phase A)

Fig. 25. Switching overvoltages at the beginning (curve m17) and at the end (curve m20a) of 30 kV cable (instant of switching in phase A)

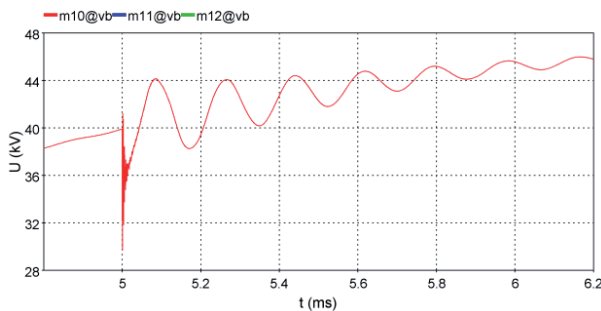

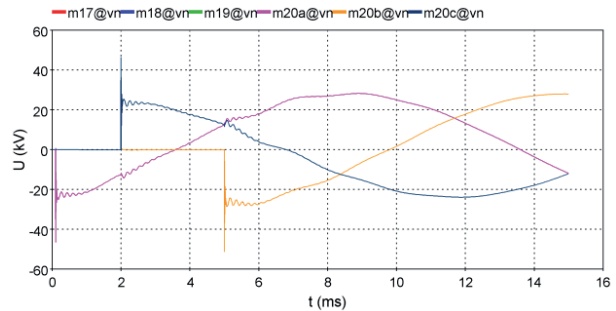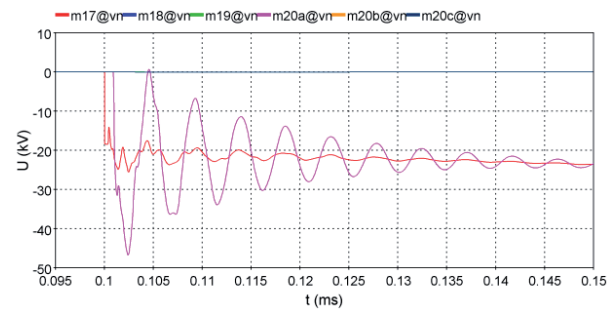Fig. 26. Switching overvoltage across tertiary winding (between phases A-B) - instant of switching in phase B
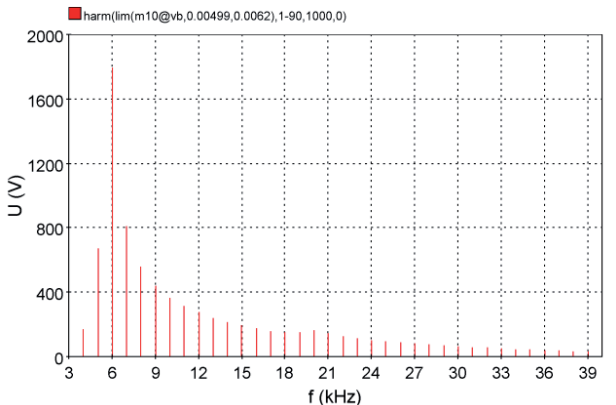

Fig. 27. LF overvoltage spectrum from Fig. 24: dominant frequency 6 kHz

Figures 22-27 show the waveforms of the calculated overvoltages and inrush currents for case B. From the results it can be concluded that there is no risk of resonant overvoltages on the tertiary winding of the transformer due to the switching of vacuum circuit breaker.

VI. Conclusion

During operation, power transformers are subjected to overvoltages that can cause failures. Therefore, it is necessary to check the amplitudes and the waveforms of overvoltages that can appear on the transformer terminals. For the analysis of fast transient phenomena, detailed models of transformers and other substation equipment (instrument transformers, surge arresters, circuit breakers etc.) are necessary.

The paper describes a high-frequency model of 400/110/30 kV power transformer with a rated power of 300 MVA, based on admittance matrix measurements. The model is verified using measurement results in the time domain. A detailed substation model is developed and an analysis of a lightning strike to a 400 kV tran-

smission line is considered near an air-insulated substation where the observed transformer is located. The transferred lightning overvoltages between the transformer primary and secondary, as well as on the tertiary winding are calculated. The paper presents an analysis of the effectiveness of overvoltage protection using surge arresters and a verification of resonant overvoltages on transformer windings. The lightning overvoltage amplitudes on all elements of the substation are within allowed limits. The overvoltage frequency spectrum and transformer winding frequency response show that no possibility of resonant overvoltages in the transformer windings exists in the analysed cases. Energy stress on the surge arresters is within allowed limits. Analysed transients include switching of a vacuum circuit breaker in a 30 kV substation connected on one side with a 400/110/30 kV power transformer via a 40 m long cable, and on the other with a neighbouring 30 kV substation via a 200 m long cable. From the results presented, it can be concluded that there is no risk of resonant overvoltages occurring on the tertiary winding of the transformer during the switching of a vacuum circuit breaker.

The transformer model described in this paper is suitable for the precise calculation of overvoltages in the grid and for the

analysis of transferred overvoltages. This can be of particular interest in the case of a transformer which has a large transformation ratio, such as larger transformers in power plants, if it needs to be determined whether the low voltage side, on which e.g. a generator can be connected, should also be protected with surge arresters. Measurements of the frequency-dependent matrix of the power transformer, from which the model is constructed, can be made relatively quickly in the factory during the production of the transformer or in the field (existing transformers that are in operation). In the case of field measurements, it is necessary to disconnect the transformer from the network. Through detailed simulations and modelling of all other components in the transformer station, it is possible to check the magnitude of the overvoltage, the effectiveness of the overvoltage protection (surge arresters) and the possibility of resonance occurring at different switching and operating conditions in the network. In this way, the occurrence of faults can be prevented, and the model enables accurate analysis of various operating events (e.g. post-mortem fault analysis, simulation of critical switching manipulations in the network, calculation of overvoltages and comparison with overvoltages recorded during operation, calculation of lightning overvoltages based on data from the lightning detection system, etc.). Simulation model presented in this paper could be used to check the potential for resonant overvoltages in the substation design stage, to check if a transformer may enter in resonance with the surrounding network (depending on different influential parameters such as cable length, transformer characteristics, etc.). In this way, appropriate measures could be implemented to avoid failures of HV equipment (for example improvement of transformer design, installation of RC snubbers, avoiding some "critical" switching operations leading to resonance, etc.).

References

[1] https://www.emtp.com/

[2] International Electrotechnical Commission, *IEC 60071-4 Insulation Co-ordination - Part 4: Computational Guide to Insulation Co-ordination and Modelling of Electrical Networks*. 2004.

[3] B. Jurišić, I. Uglesic, A. Xemard, F. Paladian, P. Guuinic, "Case study on transformer models for calculation of high frequency transmitted overvoltages", Journal of Energy, vol. 63 Number 1–4 (2014) Special Issue, p. 262-272, DOI: https://doi.org/10.37798/2014631-4186

[4] S. Keitoue, I. Murat, B. Filipovic-Grcic, A. Zupan, I. Damjanovic, I. Pavic, "Lightning caused overvoltages on power transformers recorded by on-line transient overvoltage monitoring system", Journal of Energy, vol. 67 Number 2 (2018), Special Issue, p. 44–53, DOI: https://doi.org/10.37798/201867279

[5] W. Gil, W. Masowski, P. Wronek, "Overvoltages & Transients Identification In On-line Bushing Monitoring", Journal of Energy, vol. 69 Number 3 Special Issue (2020), p. 20–24, DOI: https://doi.org/10.37798/202069340

[6] J. a. Martinez-Velasco, *Power System Transients*. United States: CRC Press, 2010. doi: 10.1201/9781420065305.

[7] CIGRÉ WG A2.37, *Transformer reliability survey*. Paris, 2015.

[8] CIGRE WG A2/C4.39, *Electrical Transient Interaction Between Transformers and the Power Systems*. CIGRE, 2013.

[9] A. Holdyk, B. Gustavsen, I. Arana, J. Holboell, and S. Member, "Wideband Modeling of Power Transformers Using Commercial sFRA Equipment," *IEEE Transactions on Power Delivery*, vol. 29, no. 3, pp. 1–8, 2014.

[10] B. Jurisic, I. Uglesic, A. Xemard, and F. Paladian, "Difficulties in High Frequency Transformer Modelling," *Electric Power Systems Research*, vol. 138, no. Special Issue: 11th International Conference on Power Systems Transients (IPST), pp. 25–32, 2016, doi: 10.1016/j.epsr.2016.02.009.

[11] B. Gustavsen, "Frequency-Dependent Modeling of Power Transformers With Ungrounded Windings," *IEEE Transactions on Power Delivery*, vol. 19, no. 3, pp. 1328–1334, 2004.

[12] Z. Ye, "Pmm: A Matlab Toolbox for Passive Macromodeling in RF/mm-Wave Circuit Design," in *2013 IEEE 10th International Conference on ASIC*, 2013, pp. 1–4. doi: 10.1109/ASICON.2013.6811857.